Dielectric Normal Mode Process of Bifurcated Linear *cis*-Polyisoprene

Hirotsugu Yoshida, Hiroshi Watanabe,* Keiichiro Adachi, and Tadao Kotaka

Department of Macromolecular Science, Faculty of Science, Osaka University, Toyonaka, Osaka 560, Japan

Received October 4, 1990; Revised Manuscript Received December 18, 1990

ABSTRACT: We examined the dielectric normal mode process of a particular type of linear *cis*-polyisoprenes (PI), referred to as *bifurcated linear PI*, which are composed of two linear PI *arms* connected in a head-to-head fashion and have dipoles along the chain contour inverted once at the center. Their behavior was compared with that of regular linear PIs without dipole inversion, and also with that of six-arm star PIs with dipoles diverging from the center to the arm ends. The relaxation time τ_n of bifurcated linear PIs was shorter by a factor of $\simeq 4$ than that of regular linear PIs with the same molecular weight, but their relaxation-mode distributions were almost the same, regardless of whether they were in the nonentangled or entangled regimes. These results are consistent with the results of normal-mode analyses on the basis of the Rouse, reptation, and/or configuration-dependent constraint release models. The behavior of six-arm star PIs was significantly different from that of bifurcated linear PIs. In the nonentangled regime, the τ_n of a six-arm star chain was nearly the same as that of a bifurcated linear chain with the same arm molecular weight M_p. However, the relaxation-mode distribution was significantly broader for the former, presumably because of a strong influence of the arm-length distribution on the Rouse–Ham eigenmodes for star chains. In the entangled regime, the τ_n was longer and the mode distribution was much broader for a six-arm star chain than for a bifurcated linear chain of the same M_p. These results suggest a difference in the dynamics of six-arm star chains in entangled and nonentangled regimes.

Introduction

Polymer chains having components of dipoles aligned in the same direction parallel to the chain contour exhibit slow dielectric relaxation processes due to their global motion.[1-6] Such a process was called the dielectric *normal mode* process.[6] Dielectric study on these polymer chains, classified as type-A chains by Stockmayer,[1] provides us very useful information on polymer dynamics.[1-16]

Adachi and Kotaka found that *cis*-polyisoprene (PI) is one of such type-A polymers and have examined extensively the dielectric behavior of linear PI chains.[7-12] The results obtained were interpreted in terms of the Rouse theory[17] for the nonentangled regime and of the reptation theory[18,19] for the entangled regime.

Dielectric spectroscopy is useful also for branched type-A chains.[4,6,13,14] Some studies have been made on star PI chains having arms of nearly the same length with the dipoles diverging from (or converting to) the junction point.[13,14] In a previous paper,[13] we compared the dielectric normal mode processes of *six-arm star* PI (6S-PI) and linear PI chains and found the following significant differences: In a lightly to moderately entangled regime, the molecular weight dependence of the relaxation time was stronger for 6S-PI chains than for linear PI chains, and the relaxation-mode distribution was much broader for the former. Those results suggested a difference in the dynamics for star and linear chains in the entangled regime, as has been well-known from rheological measurements.[20]

Results obtained for star chains were unexpectedly complex even in the nonentangled regime: The distribution of dielectric normal modes of 6S-PI chains was still broader than that for linear PI chains, although the Rouse–Ham theory[17,21] predicts that the mode distributions should be identical for 6S-PI and linear PI if the former has *monodisperse arms*. The difference between nonentangled linear and star chains was thus attributed to an enormous sensitivity of the dielectrically active Rouse–Ham eigenmodes to the arm-length distribution.[22]

As explained above, the differences between linear and star chains were related directly to the differences in their global motion, but not necessarily to the inversion of the direction of dipoles at the junction point of the star chain. To clarify the effect of dipole inversion on dielectric normal mode processes, we prepared a particular type of linear PI chain having the direction of the dipoles being inverted once at the center of the chain contour and examined their slow dielectric relaxation behavior. These linear PI chains are referred to as *bifurcated linear* PI (BL-PI) chains and are distinguished from *regular linear* PI (L-PI) chains having dipoles aligned in the same direction from one end to the other.

The global motion of the BL-PI chains is obviously identical with that of regular L-PI chains having the same molecular weight, but the dielectric response is different because of the dipole inversion. Among the eigenmodes of the BL-PI chain, some are dielectrically enhanced but the remainder, dielectrically inert, as first demonstrated by Stockmayer and Baur.[1-3] These BL-PI chains are thus ideal to isolate and examine the effect of the dipole inversion on the dielectric relaxation.

Baur and Stockmayer examined the dielectric relaxation of bulk bifurcated linear poly(propylene oxide) in the nonentangled regime,[1,3] and Pfannemüller et al. investigated the behavior of dilute solutions of bifurcated linear amylose tricarbanilate.[16] Those results were interpreted in terms of Rouse–Zimm theory.[17,23] In this paper, we compare the dielectric normal-mode processes of bulk BL- and L-PI chains in a wide range of molecular weights and discuss the results in terms of the Rouse[17] and reptation[19] models as well as of the configuration-dependent constraint release model recently proposed by Watanabe and Tirrell.[24] The behavior of the BL- and 6S-PI chains is also compared and the difference is discussed.

Experimental Section

Materials. BL-PI samples were prepared via living anionic polymerization. First, living linear PI chains were prepared in heptane with *sec*-butyllithium (BuLi) or *t*-BuLi as the initiator.

0024-9297/91/2224-2981$02.50/0

Table I
Characteristics of Bifurcated Linear *cis*-PI Samples

code	bifurcated linears $10^{-3}M_w$	M_w/M_n	precursors $10^{-3}M_p$	$(M_w/M_n)_p$
2(I-03)	5.81	1.06	2.79	1.04
2(I-05)	10.9	1.04	5.35	1.04
2(I-10)	20.9	1.03	10.4	1.04
2(I-13)	26.2	1.06	13.4	1.06
2(I-24)	47.7	1.06	23.9	1.05

An aliquot of these PI chains was taken and terminated with methanol to recover a precursor L-PI sample, which was used for characterization of BL-PI and also for subsequent dielectric measurements. The cis content of all PI chains prepared was ~75% as determined from ^{13}C NMR measurements.

After completion of the first-step polymerization, a prescribed amount of 1.5×10^{-4} mol/mL heptane solution of purified *p*-xylylene dichloride was introduced into the reactor, and ~90% of the living PI ends were coupled:

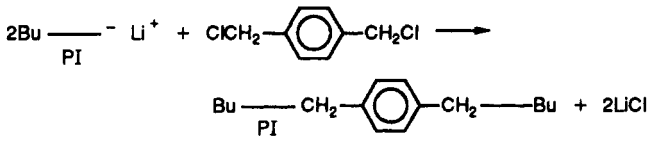

After this coupling reaction at room temperature for 1 week, the crude product was fractionated from benzene/methanol mixture to remove a small amount (≃10%) of the unreacted precursor PI chains from the BL-PI chains. The procedure was the same as in the case of fractionating 6S-PI samples.[13] After repeating the fractionation four times, we found that the precursor contaminants were thoroughly removed.

To examine the purity of the BL-PI samples obtained, we used ^1H NMR to evaluate the molar ratio of the *p*-xylylene group (coming from the coupler) and the *tert*-butyl group (from the initiator) for the shortest BL-PI chain. The ratio obtained was 0.50 ± 0.02, indicating that no precursor fragments (with the xylylene/butyl ratio = 0) were detected within the uncertainty of the NMR measurements.

The weight-average molecular weight M_w and the heterogeneity index M_w/M_n were determined on a gel permeation chromatograph (Tosoh Co., Model HLC-801A). The elution solvent was chloroform, and previously prepared L-PI samples[9,12,13] characterized by light-scattering and freezing point depression methods were used as the elution standards.

Table I summarizes the characteristics of BL-PI samples used. In the following, these samples are coded as 2(I-M_p) with the code number M_p indicating the precursor molecular weight in units of a thousand. M_p indicates the length of the chain contour through which dipoles are aligned in the same direction. This portion of the contour is referred to as the *arm* for BL-PI chains. L-PI and 6S-PI chains used are represented by I-M and 6(I-M_p), respectively, with M and M_p being the total and arm molecular weights in units of a thousand.

Dielectric Measurement. Dielectric measurements were carried out with a transformer bridge (GR-1615A) at 225–370 K for bulk PI samples. The range of frequency examined was from 0.05 to 20 kHz. Details of the dielectric cell were described previously.[9] The time–temperature superposition principle was used to obtain master curves for complex dielectric constants ϵ^*.

Theory

The complex dielectric constant $\epsilon^* = \epsilon' - i\epsilon''$ of a system of type-A chains is written as[25-27]

$$\epsilon^* - \epsilon_\infty = -\Delta\epsilon \int_0^\infty \frac{d}{dt} \frac{\langle \mathbf{P}(t)\cdot\mathbf{P}(0)\rangle}{\langle \mathbf{P}(0)^2\rangle} e^{-i\omega t}\, dt \qquad (1)$$

where $\mathbf{P}(t)$ is the polarization of the system, ϵ_∞ the unrelaxed dielectric constant, $\Delta\epsilon$ the relaxation strength, ω (= $2\pi f$) the angular frequency, and $i^2 = -1$. For bulk PI systems, Adachi and Kotaka suggested that the autocorrelation function $\langle \mathbf{P}(t)\cdot\mathbf{P}(0)\rangle / \langle \mathbf{P}(0)^2\rangle$ for the normal-mode process is attributed to the time evolution of the configuration of respective chains.[8] On the basis of this simplification, the autocorrelation function is reduced to the function for a single chain.

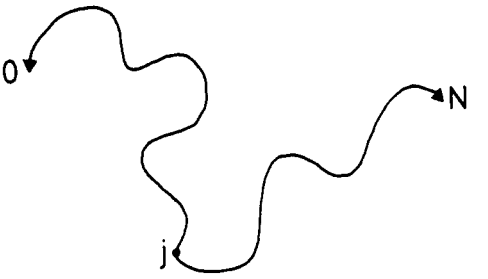

Figure 1. Schematic illustration of a bifurcated linear chain. The direction of the dipole is inverted at the jth segment.

Linear Chain. We consider a bifurcated linear PI chain composed of N segments, as indicated schematically in Figure 1. For general cases, the direction of the dipoles is assumed to be inverted at the jth segment ($0 \le j \le N$). Then ϵ^* (eq 1) is calculated as follows.

Let $\mathbf{R}(n,t)$ be the spatial position of the nth segment at time t. In a continuous limit, the polarization $\mathbf{P}(t)$ of the chain at time t is given by

$$\mathbf{P}(t) = \mu\left[-\int_0^j dn \frac{\partial \mathbf{R}(n,t)}{\partial n} + \int_j^N dn \frac{\partial \mathbf{R}(n,t)}{\partial n}\right] \qquad (2)$$

where μ is the dipole moment per segment. From eq 2, we have

$$\frac{\langle \mathbf{P}(t)\cdot\mathbf{P}(0)\rangle}{\mu^2} = \left[\int_0^j dn \int_0^j dm - \int_0^j dn \int_j^N dm - \int_j^N dn \int_0^j dm + \int_j^N dn \int_j^N dm\right] G(n,m;t) \qquad (3)$$

Here $G(n,m;t)$ is the tangent–vector correlation function defined by

$$G(n,m;t) = \left\langle \frac{\partial \mathbf{R}(n,t)}{\partial n} \cdot \frac{\partial \mathbf{R}(m,0)}{\partial m} \right\rangle \qquad (4)$$

$G(n,m;t)$ is dependent on the molecular motion. The Rouse model[17] for nonentangled chains and reptation model[19] for entangled chains lead to the same functional form of $G(n,m;t)$:

$$G(n,m;t) = \sum_p \frac{2a^2}{N} \sin\frac{p\pi n}{N} \sin\frac{p\pi m}{N} \exp(-t/\tau_1 p^{-2}) \qquad (5)$$

where a is the segment size, and τ_1 is the longest relaxation time. τ_1 is proportional to N^2 and N^3 for the Rouse and reptation models, respectively.

Within the framework of the generalized tube model, Watanabe and Tirrell[24] considered a constraint release (CR) mechanism inducing a Rouse-like motion of a tube and proposed a model for combined CR plus reptation processes for entangled polymers. Their model, referred to as the configuration-dependent constraint release (CDCR) model,[24] also leads to $G(n,m;t)$ given by eq 5. The N dependence of τ_1 for that model approaches N^3 with increasing N, but can be approximated by $N^{3.4}$ for lightly to moderately entangled chains.

From eqs 1–5, we see that the Rouse, reptation, and CDCR models all lead to

$$\epsilon_0''(\omega j,\tau_1) = \Delta\epsilon\sum_p g_p \frac{\omega\tau_1 p^{-2}}{1+\omega^2\tau_1^2 p^{-4}} \quad (6)$$

$$g_p = \frac{8}{p^2\pi^2}\left(\cos\frac{p\pi j}{N} - \frac{1+\cos p\pi}{2}\right)^2 \quad (6')$$

for a BL-PI chain with dipole inversion at the jth segment. The result for the Rouse model was first obtained by Stockmayer.[1]

For some ideal cases, eq 6 is simplified: For BL-PI chains with dipoles inverted exactly at the center of the chain ($j = N/2$), eq 6 becomes

$$\epsilon'' = \Delta\epsilon\sum_{p:\text{odd}} \frac{8}{p^2\pi^2}\frac{\omega(\tau_1/4)p^{-2}}{1+\omega^2(\tau_1/4)^2p^{-4}} \quad (7)$$

For the narrow molecular weight distribution (MWD) BL-PI chains used in this study, the distribution of j is small and eq 7 would be a good approximation. On the other hand, for regular L-PI chains without dipole inversion, j is 0 or N so that eq 6 becomes

$$\epsilon'' = \Delta\epsilon\sum_{p:\text{odd}} \frac{8}{p^2\pi^2}\frac{\omega\tau_1 p^{-2}}{1+\omega^2\tau_1^2 p^{-4}} \quad (8)$$

As seen from eqs 7 and 8, the Rouse, reptation, and CDCR models all predict that the distribution of the dielectric normal modes (observed as the shape of ϵ'' curves) for ideal monodisperse BL-PI chains (with $j = N/2$) is the same as that of monodisperse L-PI chains. In particular, the peak frequency f_m for the ϵ'' curve is predicted to be higher by a factor of 4 for the BL-PI than for the L-PI chain, both having the same molecular weight.

For a very detailed examination on the dielectric normal mode distribution of the linear PI chains used, we may need minor corrections for small distributions of molecular weight and arm length (or location of the dipole-inversion point), as explained in the Appendix. We briefly discuss these corrections later in Figure 4.

Nonentangled Star Chain. In the nonentangled region, the Rouse–Ham model[17,21] can be used to describe the slow dynamics of star chains. For an ideal type-A star chain composed of f (≥ 3) identical arms *with the length* $N/2$ (and thus the span length N), the ϵ'' curve is given by[1,4,22]

$$\epsilon'' = \Delta\epsilon\sum_{p:\text{odd}} \frac{8}{p^2\pi^2}\frac{\omega(\tau_1/4)p^{-2}}{1+\omega^2(\tau_1/4)^2p^{-4}} \quad (7')$$

τ_1 ($\propto N^2$) in eq 7′ is identical to τ_1 of nonentangled BL- and L-chains of the length N (eqs 7 and 8). Note that ϵ'' for the ideal star chains is determined by the arm length, and the arm number f is not explicitly involved in eq 7′.

From eqs 7 and 7′, we note that ϵ'' of the *ideal* 6S-PI chains is identical with ϵ'' of the *ideal* BL-PI chain of the length N. However, for *real* (nonideal) multiarm star chains, the arm-length distribution (ALD) is very important because of a high sensitivity of the Rouse–Ham eigenmodes to ALD.[22]

Results and Discussion

Molecular Weight Dependence of the Normal-Mode Relaxation Time. The relaxation time τ_n for the normal-mode process is evaluated by $\tau_n = 1/(2\pi f_m)$ with f_m being the loss peak frequency. When the dielectric-mode distribution, i.e., the shape of the ϵ'' curves, is the same for the PI chains to be compared, a comparison of τ_n evaluated from the loss peak location corresponds to the comparison of the dielectrically observed longest relaxation times.[13]

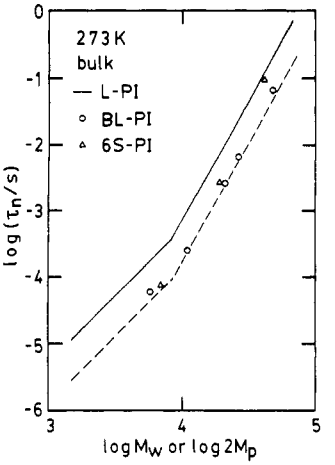

Figure 2. Molecular weight dependence of the relaxation time τ_n for the normal-mode process at 273 K in the bulk state for BL-PI chains (○). The solid line represents τ_n of L-PI reduced at an isofriction state.[12] The dashed line represents $^1/_4$ of the τ_n of L-PI chains. The data for 6S-PI (△) are plotted against the span molecular weight $2M_p$.[13]

Figure 2 shows the molecular weight dependence of τ_n for BL-PI chains in the bulk state at 273 K. The previously obtained data for L- and 6S-PI chains[12,13] are also shown for comparison. For the 6S-PI chains, τ_n is plotted against the span molecular weight $2M_p$.[13] For τ_n of L-PI chains with small M_w (<5000), correction for the free volume (segmental friction) was made.[12]

In Figure 2, we note that the τ_n for BL-PI chains (circles) are well described by the dashed line that indicates $^1/_4$ of the τ_n of the L-PI chains. As demonstrated later in Figure 3, the ϵ'' curves of BL- and L-PI chains have an (almost) identical shape, i.e., the mode distribution is (almost) the same. Thus, the comparison of τ_n for the BL- and L-PI chains suggests that all Rouse,[17] reptation,[19] and CDCR[24] models for the ideal cases (eqs 7 and 8) give a good description for the *ratio* of τ_n for the BL-PI and L-PI chains examined here.

In Figure 2, we also note that τ_n for a 6S-PI chain with the arm molecular weight $M_p < 2M_e$ (with $M_e = 5000$ being the entanglement spacing) is close to τ_n of the BL-PI chain having the same M_p. This result is superficially consistent with the prediction of the Rouse–Ham model for the ideal chains (eqs 7 and 7′). However, as demonstrated later in Figure 3, the relaxation-mode distribution is much broader for 6S-PI chains than those for BL-PI and L-PI chains. Thus, the above agreement of τ_n for short 6S-PI and BL-PI chains should be interpreted to be *qualitative*.

For star chains with $M_p \simeq 4M_e$, τ_n of the 6S-PI chain is considerably longer than that of the corresponding BL-PI chain, as seen in Figure 2. This result appears to correspond to the viscosity enhancement of star chains,[20] although the arms of the 6S-PI chains examined are not long enough to clearly exhibit an exponential increase of the viscosity with M_p. The findings for 6S-PI chains, the strong M_p dependence of τ_n (Figure 2), and the broadening of the ϵ'' curve with increasing M_p (Figure 4 in ref 13) suggest that the dynamics is not the same for short- and long-arm 6S-PI chains. Obviously the Rouse–Ham dynamics completely fails to describe the behavior of 6S-PI chains with long arms in the moderately entangled region.

Distribution of Normal Modes. Figure 3 compares the normalized ϵ'' curves, i.e., the mode distribution at

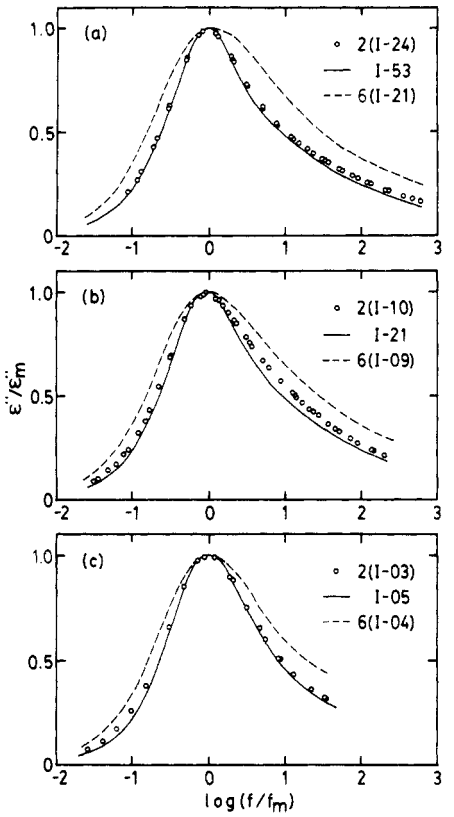

Figure 3. Comparison of normalized ϵ'' curves for narrow MWD bulk BL-, L-, and 6S-PI samples. Key: (a) 2(I-24), I-53 (M_w = 52.9 × 10³, from ref 9), and 6(I-21) (M_p = 20.7 × 10³, from ref 13); (b) 2(I-10), I-21 (M_w = 20.7 × 10³, from ref 13), and 6(I-09) (M_p = 9.49 × 10³, from ref 13); (c) 2(I-03), I-05 (M_w = 5.35 × 10³, this work; the precursor of the 2(I-05) sample), and 6(I-04) (M_p = 3.5 × 10³, from ref 13).

low frequencies for BL-PI (circles), L-PI (solid curves), and 6S-PI (dashed curves) chains, all having nearly the same span molecular weight (the total molecular weight for the first two cases). Since the characteristic molecular weight M_c for bulk PI is 10 000, parts a and b of Figure 3 represent the data in the entangled regime, and part c, those in the nonentangled regime where the Rouse–Ham model is expected to be valid.

As can be seen in Figure 3, in particular in parts a and c, BL-PI and the corresponding L-PI have ϵ'' curves of almost the same shape. This is consistent with the prediction of the models for ideal cases (eqs 7 and 8). However, we see that 6S-PI exhibits much broader ϵ'' curves even in the nonentangled regime. Thus, the Rouse–Ham model for ideal cases cannot describe the behavior of real 6S-PI chains even in the nonentangled regime. This may be due to the arm-length distribution (ALD).

As demonstrated in the previous paper,[22] a small ALD rather drastically changes the dielectrically active Rouse–Ham eigenfunctions for multiarm star chains. This makes a contrast between 6S- and BL-PI. For the latter, the ALD, i.e., the distribution of dipole-inversion points, changes the dielectric intensity factors, g_p in eq 6′, but does not affect the Rouse–Ham eigenfunctions themselves. This explains the experimental fact that the difference between the mode distributions for BL- and L-PI chains is much less significant as compared with that for 6S- and L-PI chains (Figure 3).

In this connection, we see a small difference of the dielectric relaxation mode distribution between the 2(I-10) and I-21 chains in the part b of Figure 3. Also, for parts a and c, a detailed inspection may suggest a slight

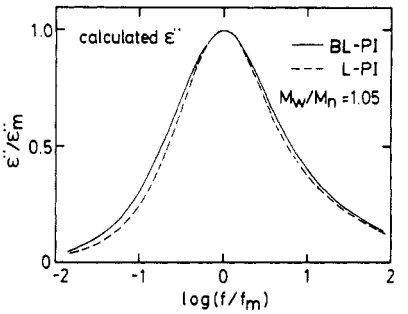

Figure 4. Comparison of the ϵ'' curves calculated for BL-PI (solid curve) and L-PI (dashed curve) chains with the same MWD, M_w/M_n = 1.05. For the former, a distribution of the arm length is also taken into account (eqs A-1 and A-2).

difference, although much less significant than that found in part b. Small but finite MWD and ALD of the L- and BL-PI samples, which may be somewhat different from a sample to sample, could be responsible for the small differences in the dielectric relaxation mode distribution of BL- and L-PI chains found in Figure 3. As explained in the Appendix, we made a model calculation on nonentangled BL- and L-PI chains with the same MWD (M_w/M_n = 1.05) to estimate the effects of MWD and ALD on the mode distribution. As demonstrated in Figure 4, MWD and ALD may lead to a small difference in the shape of the ϵ'' curves of the BL- and L-PI chains, which is comparable to that observed in Figure 3b. However, for BL- and L-PI chains with narrow ALD and MWD, the difference is small in any case and is not important unless we are making a very detailed discussion.

Finally, we have to point out that the Rouse, reptation, and CDCR models (eq 6) do not exactly describe the shape of ϵ'' curves *in the entire range of frequencies*.[28] At low frequencies, $f \leq 10f_m$, the models with MWD can describe ϵ'' well.[28] However, they underestimate ϵ'' at higher frequencies. All those models are the models for slow relaxation and become a poorer approximation for faster modes. This problem is further discussed in our forthcoming paper.[28]

Conclusions

We have found that the relaxation time τ_n of the dielectric normal mode process for BL-PI is close to $^1/_4$ of that for the corresponding L-PI with the same molecular weight (Figure 2), and that the relaxation-mode distribution is almost the same for BL-PI and L-PI (Figure 3). These features are consistent with the results of normal-mode analyses on the basis of the Rouse, reptation, and CDCR models for BL-PI chains composed of identical arms.

For nonentangled 6S-PI and BL-PI chains having the same arm molecular weights, we have found that τ_n is nearly the same but the relaxation-mode distribution is significantly broader for the former (Figures 2 and 3). The broad mode distribution of the 6S-PI chains may be due to their arm-length distribution (ALD), and the Rouse–Ham model without ALD (eq 7′) can be used only in a qualitative way to interpret the data. On the other hand, in a moderately entangled regime, τ_n is considerably longer and the mode distribution is much broader for 6S-PI than for BL-PI having the same M_p. These differences suggest a difference in the dynamics of entangled and nonentangled star chains, the former no longer obeying the Rouse–Ham dynamics in any sense.

Appendix

Effect of Arm-Length Distribution on the ϵ'' Curve for Bifurcated Linear Chains. In the nonentangled

region, τ_1 in eq 6 is written as $\tau_0 N^2$ with τ_0 being a constant independent of N and j.[12] From eq 6, ϵ'' for a BL-PI chain with MWD and ALD is given by

$$\epsilon'' = \int dN \int dj\, P_w(N,j)\epsilon_0''(\omega, j, \tau_0 N^2) \qquad \text{(A-1)}$$

Here $P_w(N,j)$ is the weight fraction of a BL-PI chain with the left and right arms composed of j and $N - j$ segments, respectively (cf. Figure 1). Assuming that a BL-PI sample was prepared through a random coupling of living PI precursors with a Schulz–Zimm distribution, we approximated $P_w(N,j)$ for the BL-PI chain by

$$P_w(N,j) = \frac{N\beta^{2\alpha+1}(jN - j^2)^{\alpha-1}e^{-\beta N}}{2\Gamma(\alpha+1)\Gamma(\alpha)} \qquad \text{(A-2)}$$

The constant α is estimated from M_w/M_n ($=(2\alpha+1)/2\alpha$), and $\Gamma(x)$ is the Γ function of x. The shape of the ϵ'' curve calculated from eqs A-1 and A-2 does not depend on the constant $\beta = (2\alpha+1)/N_w$, with N_w being the weight-average segment number. For regular L-PI chains with MWD, ϵ'' is calculated also by eq A-1, except that $j = 0$ (or N) and P_w is given by a usual Schulz–Zimm distribution. The results of a model calculation for nonentangled BL- and L-PI chains with the same MWD ($M_w/M_n = 1.05$) are demonstrated in Figure 4.

References and Notes

(1) Stockmayer, W. H. *Pure Appl. Chem.* **1967**, *15*, 539.
(2) Stockmayer, W. H.; Baur, M. E. *J. Am. Chem. Soc.* **1964**, *86*, 3485.
(3) Baur, M. E.; Stockmayer, W. H. *J. Chem. Phys.* **1965**, *43*, 4319.
(4) Stockmayer, W. H.; Burke, J. J. *Macromolecules* **1969**, *2*, 647.
(5) North, A. M. *Chem. Soc. Rev.* **1972**, *1*, 49.
(6) Adachi, K.; Kotaka, T. *Macromolecules* **1983**, *16*, 1936.
(7) Adachi, K.; Kotaka, T. *Macromolecules* **1987**, *20*, 2018.
(8) Adachi, K.; Kotaka, T. *Macromolecules* **1988**, *21*, 157.
(9) Imanishi, Y.; Adachi, K.; Kotaka, T. *J. Chem. Phys.* **1988**, *89*, 7585.
(10) Adachi, K.; Imanishi, Y.; Kotaka, T. *J. Chem. Soc., Faraday Trans. 1* **1989**, *85*, 1065, 1075, 1083.
(11) Adachi, K.; Itoh, S.; Nishi, I.; Kotaka, T. *Macromolecules* **1990**, *23*, 2554.
(12) Adachi, K.; Yoshida, H.; Fukui, F.; Kotaka, T. *Macromolecules* **1990**, *23*, 3138.
(13) Yoshida, H.; Adachi, K.; Watanabe, H.; Kotaka, T. *Polym. J.* **1989**, *21*, 863.
(14) Boese, D.; Kremer, F.; Fetters, L. J. *Makromol. Chem., Rapid Commun.* **1988**, *9*, 367; *Macromolecules* **1990**, *23*, 1826.
(15) Boese, D.; Kremer, F. *Macromolecules* **1990**, *23*, 829.
(16) Pfannemüller, B.; Schmidt, M.; Ziegast, G.; Matsuo, K. *Macromolecules* **1984**, *17*, 710.
(17) Rouse, P. E. *J. Chem. Phys.* **1953**, *21*, 1272.
(18) de Gennes, P.-G. *J. Chem. Phys.* **1971**, *55*, 572.
(19) Doi, M.; Edwards, S. F. *The Theory of Polymer Dynamics*; Clarendon Press: Oxford, 1986.
(20) See, for example: Graessley, W. W.; Roovers, J. *Macromolecules* **1979**, *12*, 959.
(21) Ham, J. S. *J. Chem. Phys.* **1957**, *26*, 625.
(22) Watanabe, H.; Yoshida, H.; Kotaka, T. *Polym. J.* **1990**, *22*, 153.
(23) Zimm, B. H. *J. Chem. Phys.* **1956**, *24*, 269.
(24) Watanabe, H.; Tirrell, M. *Macromolecules* **1989**, *22*, 927.
(25) Cole, R. H. *J. Chem. Phys.* **1965**, *42*, 637.
(26) Nee, T.-H.; Zwanzig, R. *J. Chem. Phys.* **1970**, *52*, 6353.
(27) Williams, G.; Watts, D. C. *Trans. Faraday Soc.* **1970**, *66*, 80.
(28) Watanabe, H.; Yamazaki, M.; Yoshida, H.; Adachi, K.; Kotaka, T. *Macromolecules*, in press.